Degradation pattern of a porcine collagen membrane in an *in vivo* model of guided bone regeneration

Calciolari E[1,2], Ravanetti F[3], Strange A[4], Mardas N[2], Bozec L[4], Cacchioli A[3], Kostomitsopoulos N[5], Donos N[1, 2]

1. Centre for Oral Clinical Research, Institute of Dentistry, Queen Mary University of London (QMUL), Barts and The London School of Medicine and Dentistry, London, UK
2. Centre for Oral Immunobiology and Regenerative Medicine, Queen Mary University of London (QMUL), Barts and The London School of Medicine and Dentistry, London, UK
3. Department of Veterinary Science, University of Parma, Parma, Italy
4. Department of Biomaterials and Tissue Engineering, UCL Eastman Dental Institute, London, UK
5. Laboratory Animal Facilities, Biomedical Research Foundation of the Academy of Athens, Athens, Greece

Corresponding author
Dr Elena Calciolari
DDS, MS, PhD
Centre for Oral Clinical Research
Centre for Oral Immunobiology and Regenerative Medicine
Institute of Dentistry
Barts and The London School of Medicine and Dentistry
Queen Mary University of London
Turner Street
London E1 2AD
e.calciolari@qmul.ac.uk
Tel. 0207 882 6340

Abstract

Objective To investigate the degradation pattern of a porcine non-cross-linked collagen membrane in an *in vivo* model of guided bone regeneration (GBR).

Background Although collagen membranes have been clinically applied for guided tissue/bone regeneration for more than 30 years, their *in vivo* degradation pattern has never been fully clarified. A better understanding of the different stages of *in vivo* degradation of collagen membranes is extremely important, considering that the biology of bone regeneration requires the presence of a stable and cell/ tissue-occlusive barrier during the healing stages in order to ensure a predictable result.

Methods Decalcified and paraffin-embedded specimens from calvarial defects of eighteen, 10-month old Wistar rats were used. The defects were treated with a double layer of collagen membrane and a deproteinized bovine bone mineral (DBBM) particulate graft. At 7, 14 and 30 days of healing, qualitative evaluation with scanning electron microscopy (SEM) and atomic force microscopy (AFM) and histomorphometric measurements were performed. Markers of collagenase activity and bone formation were investigated with immunofluorescence technique.

Results A significant reduction of membrane thickness was observed from 7 to 30 days of healing, which was combined to a progressive loss of collagen alignment, increased collagen remodelling and progressive invasion of woven bone inside the membranes. A limited inflammatory infiltrate was observed at all healing points.

Conclusion The collagen membrane investigated was biocompatible and able to promote bone regeneration. However, pronounced signs of degradation were observed starting from day 30. Since successful regeneration is obtained only when cell occlusion and space maintenance exist for the heling time needed by the bone progenitor cells to repopulate the defect, the suitability of collagen membranes in cases where long-lasting barriers are needed, needs to be further reviewed.

Introduction

The use of a barrier membrane to promote the selective repopulation of a periodontal/bone defect by cells with a regenerative rather than reparative potential has been successfully applied for more than forty years (1). In particular, in Guided Bone Regeneration (GBR), the surgical placement of a tissue occlusive membrane has been applied for the predictable treatment of atrophic ridges, peri-implant defects, for socket preservation and for *de novo* bone formation in healthy and medically compromised conditions (2-5) (for review see (6, 7)). An ideal barrier for GBR should combine biocompatibility and tissue conclusiveness with clinical manageability, space maintenance and the possibility to gradually resorb overtime (8). Collagen forms a significant part of the body and of the connective tissue's proteins and it is continuously remodelled by specific enzymes called collagenases (9). Collagen-based membranes can be obtained from human skin, bovine Achilles tendon or porcine skin, and inner organs (10). Their advantages in comparison to non-resorbable membranes are several: a simplified one-stage surgical procedure, cost-effectiveness, decreased patient morbidity, a quick resorption in case of exposure, and an improved soft tissue healing. Nevertheless, it is difficult to predict and control the duration of maintaining occlusive properties, and this can unfavorably interfere with the bone healing process (11-13). Another disadvantage of collagen membranes is related to their unfavourable mechanical properties, which leads to collapse into the bony defects, hence their combination with a bone graft is recommended when clinically applied (14, 15).

Although the application of collagen membranes in guided bone/tissue regeneration is well established in clinical practice, surprisingly only a limited number of studies have investigated their resorption pattern and they have shown that the degradation of collagen membranes might start within 4 days to 6 weeks after surgical placement (16-18). However, in most of the published studies collagen membrane resorption was evaluated after subcutaneous implantation (17, 19-21), which does not resemble the clinical milieu, where the membrane is in direct contact with the pristine bone, the graft and the soft tissues within the context of a surgical osseous wound. Moreover, the available data mainly consists in qualitative histologic observations and/or on the measurement of the membrane thickness, with little characterization of the enzymatic degradation process (12, 16, 22).

Hence, the aim of this study was to investigate qualitatively and quantitatively the early and late degradation of a commonly used porcine collagen type I and III membrane associated to a bovine osteoconductive graft in an *in vivo* model for GBR.

Materials and Methods

This study was carried out on rat samples obtained as part of a previously approved project (23, 24). The protocol was approved by the Ethical Committee of the General Directorate for Agricultural Economy and Veterinary Medicine of Athens, Greece (protocol number 590), and was carried out in accordance with EU Directive 2010/63/EU for animal experiments. The ARRIVE guidelines for reporting animal research were followed (25).

Experimental GBR model

Eighteen 10-month old, Wistar rats were used. After two weeks of acclimatization the experimental GBR surgical procedure was performed, as previously described (23). Briefly, a standardized 5.0-mm of diameter critical size defect (CSD) was created on each parietal bone by the use of a trephine burr. A porcine collagen membrane (Geistlich Bio-Gide®, Wolhusen, Switzerland) was trimmed and adapted to the intracranial part of the defects, a deproteinized bovine bone mineral (DBBM) graft (Geistlich Bio-Oss®, Wolhusen, Switzerland) was than loosely compacted into the defect and eventually covered by a second resorbable collagen membrane (Geistlich Bio-Gide®, Wolhusen, Switzerland). The flap was sutured in layers (Vicryl® 5.0, Ethicon, Cincinnati, OH, USA). Six animals were randomly sacrificed at 7, 14 and 30 days of healing. During the sacrifice, one defect was randomly chosen for decalcified histology and one for proteomic analysis (results described in (23, 24)).

Histology analysis and histomorphometric measurements

The three most central sections of each sample were stained with hematoxylin and eosin and one section was stained with Masson trichrome staining and the following evaluations were performed by a blind, previously trained examiner with a light microscope (Olympus BX50, Olympus America, Inc., Center Valley, PA, USA) connected to a digital color camera (CoolSNAP-Pro Media Cybernetics Inc., Marlow, Buckinghamshire, UK):

1. <u>Qualitative descriptive histology</u> at different magnifications (X4, X10, X20, X40). One section of each sample was also stained with picrosirius red and qualitatively examined under polarized light. This stain allows to distinguish aligned (red) and not aligned (green) collagen fibers (26).

2. <u>General and specific tissue reaction</u>: in three regions of interest (ROI) (one at one end, one at the opposite end and one in the middle) according to Bozkurt et al (20). Details of the parameters evaluated and of the scoring system are presented in Table 1.

   <u>Thickness of the upper and lower collagen membrane (micron)</u>: measured with the help of the software Image-Pro Plus (Version 4.5.0, Media Cybernetics Inc., Marlow, Buckinghamshire, UK) at X4 magnification in three areas alongside the full length of each membrane (two at the margin of the defect and one in the middle). The mean value was calculated for the extracranial and intracranial membranes. Moreover, the thickness of an intact dry collagen membrane (DM) (Geistlich Bio-Gide®, Wolhusen, Switzerland) and of an intact collagen membrane that was processed and embedded into paraffin (PM) were measured.

Atomic force microscopy (AFM) and scanning electron microscopy (SEM)

An intact porcine collagen membrane and two randomly selected samples per healing point were qualitatively assessed with AFM and SEM. The histology sections used for AFM, were firstly stained with picrosirius red, then imaged using light microscopy to identify red, yellow and green areas. Once the areas were identified, AFM contact imaging in air was performed using Dimension 3100 and Dimension Icon AFMs (Bruker), with MSNL-10 probes. The sections used for SEM were fixed with 3% glutaraldehyde for 24 hours, dehydrated in an ethanol series, mounted on stubs and coated with gold/palladium. Sections were then imaged on a Philips XL30 FEG-SEM, with an acceleration voltage of 5kV.

Immunofluorescence analysis

The following antibodies were applied for immunofluorescence analysis on 3 randomly selected samples per group:

- MMP-1 (Bioss bs-0463R), MMP-8 (Bioss bs-1913R) and TIMP-1 (Santa Cruz Biotechnology, Inc. sc-6834) as collagenase activity markers;

- TNF-α (Bioss bs-2081R), IL-1β (Neuromics Antibodies GT15102) as inflammation markers;

- osteopontin (Bioss bs-0026R), bone sialoprotein (Bioss bs-4729R) and osteocalcin (Bioss bs-4917R) as new bone formation markers;

- Vimentin (Bioss bs-3471R) as mesenchymal cell marker.

Three sections per animal were used, in order to have triplicates of the results. The sections were treated with boiling EDTA buffer and maintained at 80 °C for 10 minutes for antigen retrieval. After reaching RT, the blocking step was carried out with 5% BSA in PBS for 30 minutes. The sections were incubated with the primary antibodies diluted 1:50 in PBS containing 5% BSA over night at 4°C. After a washing step, the secondary antibody (Jackson ImmunoResearch Laboratories) was added. Finally, the sections were stained with DAPI for 5 minutes and then were mounted with anti-fading medium. A standard DAPI-FITC-TRITC combination filter was used to assess the positivity for the aforementioned antibodies.

A semi-quantitative scoring system was applied as follows: -, when less than 10% positivity was detected; +, for ≥10% positive cells; ++, for ≥25% positive cells and +++, for ≥50% positive cells(modified from (27)).

Statistical analysis and sample size

In light of the "reduction" principle in animal research, for this project we used samples of a previously approved study that aimed at describing histologically and at a proteomic level the process of bone regeneration in healthy and osteoporotic-like rats (23, 24). Hence, sample size was not calculated based on a specific membrane degradation parameter.

Differences in membrane thickness (micron) at the different healing periods were investigated with one-way ANOVA (SPSS® software, IBM Corp. Released 2013, Version 22.0. Armonk, NY: IBM Corp.). Post-hoc Tukey test was applied to explore differences in means between the healing times. 20% of the samples were measured again the after 1 week from the first evaluation and the reproducibility was tested with the Bland and Altman diagram, the calculation of the British Standards Institution repeatability coefficient and Lin's concordance correlation coefficient. The general and specific tissue reactions, as well as the immunofluorescence markers were graphically presented in summary tables.

Results

Qualitative histology

At 7 days, the margins of the defects were clearly detectable and both collagen membranes were in place and well preserved in all specimens. The penetration of body fluids had given the membranes a "spongy" aspect, with initial separation between the collagen bundles. The most prevalent cells were erythrocytes, although a few polymorphonuclear leukocytes and lymphocytes were also identified. The picrosirius red stain showed widespread red areas in both intracranial and extracranial membranes, with only isolated green spots amongst the red fibers, thus identifying an overall aligned collagen structure (Figure 2, a and a-1).

At 14 days, initial signs of breakdown of the eosinophilic collagen bundles (especially in the upper membrane) were identified. A limited infiltrate of polymorphonuclear leukocytes, lymphocytes and macrophages was observed through the whole thickness of both intracranial and extracranial membranes. The sections stained with picrosirius showed an increasing amount or green spots within the red collagen bundles (Figure 2 b and b-1).

At 30 days, both intracranial and extracranial membranes were infiltrated by a few pyknotic cells (mainly polymorphonuclear leukocytes and lymphocytes) and marked signs of dissolution/degradation were detectable. In particular, the eosinophilic collagen bundles were fragmented in short and scattered clusters, with new vessels penetrating them. Close to the defect margins it was also possible to identify new bone formation spreading from the margins of the defect into the membranes, thus embedding the collagen fibers. The picrosirius stain confirmed a general loss of collagen register, with diffuse orange and green areas throughout the membranes and limited red areas (Figure 2 c and c-1).

General and specific tissue reaction

The general tissue reaction score showed the presence of a significant hemorrhage infiltrate both at 7 and 14 days and an increasing number of blood vessels in both intracranial and extracranial membranes from 7 to 30 days of healing (Table 1). A higher number of blood vessels was observed in the extracranial membrane, particularly at day 30.

The specific tissue reaction indicated a limited inflammatory reaction, as at neither of the healing periods we identified a score higher than 0.5, which indicates an average number of cells <10 in the regions of interest. The identified cells consisted mainly in polymorphonuclear leukocytes, lymphocytes and macrophages.

Representative histological microphotographs obtained with different histological stainings at 7, 14 and 30 days of healing are presented in Figure 3 in order to support the data presented in Table 1.

Membrane thickness

The thickness of both intracranial and extracranial membranes significantly reduced from 7 to 30 days of healing (Figure 1).

Although the extracranial membrane tended to present a reduced thickness in comparison to the intracranial one, this trend was not statistically significant. In comparison to the intact control sample processed and embedded into paraffin (PM), both extracranial and intracranial membranes showed an increased thickness at 7 day, that reduced to approximately the same thickness of PM at 14, and then further reduced at 30 days of healing. The reproducibility of the measurements was fairly accurate, with a non-statistically significant difference between the first and second readings of $\bar{d}$ = -0.005 mm (SD 0.014 mm) for the extracranial membrane and of $\bar{d}$ = -0.011 mm (SD 0.019 mm) for the intracranial membrane. The British Standards Institution repeatability coefficient was 0.028 mm and 0.038 mm, respectively and the Lin's correlation coefficient was 0.997 (95% CI 0.991-0.999) and 0.996 (95% CI 0.986-0.999), respectively.

AFM and SEM

At day 7, only a loose collagen network could be seen in both extracranial and intracranial membranes at SEM. This network was highly porous with thin fibrils, but a large infiltration of erythrocytes and limited neutrophils was present (Figure 4a). The AFM returned an irregular picture, but it was possible to identify areas where collagen bundles were still visible (Figure 3d)

At day 14, a less porous collagen network was observed, with an increase in the quantity of fibrils. Erythrocytes were still present and embedding both membranes (Figure 4b). Remarkably, collagen fibrils were also organizing around the graft particles inside the defect area.

At day 30, the collagen network size had increased again in both membranes, with few pores observed. Infiltration of various cell types was observed, with signs of colliquation of the collage membranes (Figure 4c). At high magnification, it was impossible to distinguish the

peculiar collagen bundle structure, but both membranes were infiltrated by areas of mineralization and what appeared as a denser tissue network.

AFM pictures at 14 and 30 days did not provide good quality data, owing to the irregular surface of the samples, and It was impossible to identify collagen fibrils.

Immunofluorescence analysis

The markers of collagenase activity (MMP-1, MMP-8 and TIMP-1) showed no positivity at day 7, whilst punctiform positivity was detected at day 14, which significantly increased at day 30 (Figure 5). On average, at 14 days, $\geq$10% of cells were positive to MMP-1 and TIMP-1 within the defect area, while $\geq$ 25% cells were positive to MMP-1 and MMP-8 and $\geq$10% of cells were positive to TIMP- within the membranes. At 30 days, the positivity to collagenase markers further increased within the membranes, with $\geq$50% of cells positive to MMP-1 and $\geq$ 25% cells positive to MMP-8 (Table 2). The positivity was mainly observed in proximity to the membrane elastic fibers.

Markers of inflammation (TNF-α and IL-1β) were not detected (or <10% of positive cells) neither in the membranes nor in the defect area at all healing periods (Table 2).

Markers of bone formation were identified starting from day 14 both in the defect and within the membranes (Figure 6). At 14 days, $\geq$ 10% cells within the defect were positive to osteopontin and osteocalcin, whist $\geq$ 25% cells were positive to bone sialoprotein. At 30 days, $\geq$ 10% cells within the defect were positive to osteopontin and $\geq$ 20% cells were positive to bone sialoprotein and osteocalcin (Table 2). In the defect area, most of the fluorescent spots were identified in close proximity to the DBBM graft particles. In the membranes, the positivity started at 14 days and reached the highest scores at 30 days for all markers, when $\geq$ 20% cells were positive to bone sialoprotein and osteopontin and $\geq$ 10% cells were positive to osteocalcin (Table 2).

Vimentin was expressed in the defect area in $\geq$10% of the cells at day 14, whilst at 30 days a moderate positivity ($\geq$10% cells) was found in the membrane area (Table 2).

Discussion

The porcine type I and III collagen membrane adopted was biocompatible and inert, did not elicit an inflammatory or foreign body reaction, and was able to positively promote the bone

regeneration process. Membrane integrity was well maintained during the first 14 days, but at 30 days pronounced signs of degradation, high levels of remodeling and a significant reduction in thickness were identified. These data confirm previous findings in a similar model from Moses et al (22) that showed a significant reduction in membrane thickness from 14 to 30 days of healing, as well as a significant reduction in the total amount of collagen. Remarkably, at 30 days, bone formation markers (ALP, BS, OPN), mesenchymal cell marker (Vimentin) and histology features suggested that bone formation was spreading inside the membranes and embedding the fragmented collagen bundles. While this implies a loss of integrity as a barrier, at the same time the membrane was able to support the bone regeneration process (23) and to create an environment that promoted the deposition and mineralization of the bone matrix, with blood vessels penetrating throughout the membrane at 30 days. A recent study in a similar calvaria defect model also confirmed that, at 30 days of healing, the collagen membrane network is progressively invaded by areas of bone formation and presents a dense infiltrate of leukocytes and fibroblast-like cells (28).

The trend for a higher resorption of the extracranial compared to the intracranial membrane observed in our study might be justified by the increased number of blood vessels detected in the extracranial barrier. The vessels originating by the overlaying periosteum and inner skin might have, in fact, contributed to accelerate the resorption of the extracranial barriers. Our results are in line with previous studies reporting that the porous structure of non-cross-linked collagen membranes is suitable for the formation of trans-membrane blood vessels, which may also facilitate membrane resorption (12, 21, 29). Recently, Turri et al have also shown that collagen membranes act as bioactive compartments rather than passive barriers, as they are involved in attracting cells into the wound area, which secrete signals for bone regeneration and remodeling, and they promote the expression of chemotactic factors, thus modulating the overall osteogenic process (30).

Throughout the SEM images taken of the collagen membrane, a clear pattern of healing could be observed from 7 to 30 days. Firstly, the collagen network increased in size, with individual fibrils being harder to see as the network grew and the porosity reduced. The increase in the amount of collagen could be linked to the recovery and maturation of the wound area, as it went in parallel with the progressive increase in the amount of bone formation and maturation of the newly formed bone (histomorphometric data presented in (23)). Secondly, the apparent cell makeup in the network changed over time. Initially, there was a large

contribution from erythrocytes, but as the healing progressed, more leukocytes, eosinophils and neutrophils were detected at the healing site.

The collagen remodelling was confirmed by the immunodetection of Matrix Metalloproteinases (MMP) 1 and 8. The remodelling process is necessary for the wound healing process. Leukocytes, particularly macrophages and neutrophils, are major sources of MMP production (31, 32). Other cells involved in the postacute stages of wound healing can also contribute to MMP release, such as fibroblasts and endothelial cells (33). Most MMPs are not constitutively expressed in normal tissues, but inflammatory cytokines, such as IL-1 and TNF, or growth factors, such as TGF-beta, and noxious stimuli are required to initiate the transcription (34-36). In this study, the high positivity for MMP-1, MMP-8 and TIMP-1 found at the later healing periods was not associated to a high inflammatory infiltrate, and the IL-1β and TNF-α markers did not return significant positivity (or a positivity <10%) at all healing times. The lack (or low) of positivity for IL-1β and TNF-α might be related to the sample processing. It is well-known that the decalcification and processing of the samples are antigen masking (37) and that different antigens may show immunoreactivity differences in relation to time and preservation of the samples (38), so it is possible that a weak positivity for inflammatory markers might have been concealed or, at least reduced. Previous studies have also shown that osteoblasts and osteocytes express MMPs and TIMP1 in the course of appositional bone formation (39), so our data on MMPs expression at 14 and 30 days also suggest a maturing osseous wound.

Since a control group without bone graft particles was not present, we do not know if the graft influenced collagen barrier degradation in terms of MMP expression. Previously, Elgali et al (40) tested the early events of bone healing and the cellular activities in response to a combination of GBR membrane and different bone substitute materials. No data about MMP activity was reported, but the study showed that the defects treated with a collagen membrane and the defects treated with a combination of collagen membrane and deporteinized bovine bone had similar expression of osteoclasts and inflammatory markers. Only at 12 hours it was possible to detect a temporary higher expression of RANKL in the defects covered only by the membrane and a higher expression of TNF-α in the defects where the graft was also applied. However, at later healing points no significant differences were detected.

To the best of our knowledge, this is the first study that thoroughly evaluated the degradation of a collagen membrane by qualitative histology, by qualitative SEM and AFM evaluations, by antigen-antibody characterizations and histomorphometry in an *in vivo* model that is a close approximation of the clinical scenario where this membrane is commonly applied and in combination with a particulate bone graft. Previously, Rothamel et al (18) studied the degradation of two collagen membranes associated to different bovine bone grafts. The authors only performed qualitative histological and SEM observations, but their results are in line with ours in terms of low inflammatory reaction, early vascularization and limited cell proliferation

DBBM has been successfully applied in combination with membranes in numerous human bone regeneration and augmentation studies (3, 41-44). The use of DBBM does not enhance *per se* the capacity of the membrane to promote bone formation, but it demonstrates osteoconductive properties and mechanically supports/provides space maintenance to the barrier against its collapse into the defect (45, 46). In the current project, the marked positivity to osteopontin, bone sialoprotein and osteocalcin around the DBBM particles corroborated the osteoconductivity of this graft.

In clinical practice, successful regeneration is obtained only when cell occlusion and space maintenance exist for the heling time needed by the progenitor cells to repopulate the defect. While in periodontal regeneration a period of 6 to 8 weeks might be sufficient (47), a longer period up to 6 months has been advocated for bone regeneration (48, 49). Hence, future studies considering longer healing periods are warranted to test the degradation process of collagen membranes in GBR models.

Nevertheless, good long-term clinical results have been documented when collagen membranes without a prolonged barrier function were combined with autologous bone chips and DBBM for contour augmentation around chemically modified, sandblasted and acid-etched implants (50). Therefore, the use of the porcine collagen membrane tested in this study in GBR needs to be reviewed in light of the new implant surfaces and biomaterials adopted and in relation to the clinical application (GBR around implants, for socket preservation, or for the regeneration of atrophic ridges).

In order to increase the stability of collagen membranes and delay their degradation, different approaches have been proposed, including cross-linking the collagen (51), applying a double layer of membranes (12), using tetracycline impregnation (52, 53) and systemically

administering tetracycline (54). By modifying surface properties, particle size, porosity and the release of ions, future studies should aim at manufacturing an ideal immune-mediated collagen membrane that promotes anti-inflammatory M2 macrophages and the secretion of regenerative cytokines, whilst at the same time prevents the migration of undesired soft tissues into the osseous wound (55).

The combined approach proposed in the current project to assess membrane degradation (quantitative and qualitative histology, immunofluorescence, SEM/AFM) allowed a thorough *in vivo* characterization of collagen degradation and might be successfully used in the future to test the behavior of other barrier membranes (e.g. cross-linked collagen membranes). Longer healing times are advised in future studies, in consideration of the long-lasting barrier effect advocated for GBR.

Finally, this study investigated barrier degradation during an uneventful healing process. However, in clinical practice it is not uncommon to observe membrane exposure (56), especially during the early healing stages. As the membrane becomes exposed to the oral environment, bacterial enzymatic products and saliva enzymes will trigger a faster degradation of the biomaterial, with the possibility that the bacterial colonization of the membrane may compromise the final regeneration outcome (57-61). In the future, it would be interesting to apply the methodologies developed in this study to investigate also how the exposure to the oral environment might influence membrane properties and degradation.

Figure legend

Figure 1 The mean thickness (micron) and standard deviation of the extracranial membrane (EM) and intracranial membrane (IM) at the different healing times are graphically presented. The thickness of an intact dry membrane (DM) and of a processed membrane (PM) are also shown. ∗ indicates significant difference in comparison to 7 days of healing; ╱ indicates significant difference in comparison to 14 days of healing.

Figure 2 Sections stained with picrosirius red. a, a-1, 7-day healing section. At this early healing period, both membranes presented aligned (red) collagen. b, b-1, 14-day healing section. At this healing time, some green dots were detectable inside the red membrane. c, c-1, 30-day healing section. At this later time point, the membrane was almost entirely replaced by either non-aligned collagen or a loose granulation tissue resembling woven bone. Widespread areas of orange and green were clearly detectable inside both membranes.

Figure 3 Representative histological microphotographs at 7, 14 and 30 days after surgery. a, b, c: giemsa staining of samples at the different healing period (asterisks indicate fatty infiltrates). d, e, f: masson trichrome staining at different healing period (arrows indicate blood vessels; arrowheads indicate extravasated erythrocytes). G, g, i: hematoxylin and eosin staining (circular arrowheads indicate inflammatory infiltrate). Scale bar 100 micron.

Figure 4 a, section of 7-days healing period at SEM. At this stage, a loose network of collagen fibers was detected, which were infiltrated mainly by erythrocytes and a few polymorphonuclear leukocytes and lymphocytes. b, section of 14-days healing period at SEM. A more organized network of fibers and cells was detected. c, section of 30-days healing period at SEM. Signs of colliquation of the membrane (arrows) and infiltration by different cell types were observed. d, Section of 7-days healing period at AFM. The image was taken in a "red" area of a section stained with picrosirius red. We can foresee the bundle structure of collagen in some areas (arrows), although overall the surface was very irregular and did not allow for good quality pictures.

Figure 5 a, d, Immunofluorescent spots indicate cells positive for MMP-1 at 14 (a) and 30 (d) days. b, e, Immunofluorescent spots indicate cells positive for MMP-8 at 14 (b) and 30 (e)

days. c, f, Immunofluorescent spots indicate cells positive for TIMP-1 at 14 and 30 days. All markers are identifiable in TRITC.

Figure 6 a, Immunofluorescent spots indicate cells positive for osteopontin (OPN) at 30 days (identifiable in TRITC). b, Immunofluorescent spots indicate cells positive for osteocalcin (OC) at 14 days (identifiable in TRITC). c, Immunofluorescent spots indicate cells positive for bone sialoprotein (BSP) at 30 days (identifiable in FITC).

Table legend

Table 1 Average details of the general and specific tissue reaction scores according to Bozkurt et al (20). The general tissue reaction was evaluated according to the following scoring system: - = not present; + = present in ≥10% of the viewed area, ++ = present in ≥20% of the viewed area and +++ = present in ≥50% of the viewed area. The number of blood vessels (and standard error, SE) in the extracranial and intracranial membranes of each sample was counted. The specific tissue reaction was evaluated according to the following scoring system: 0 = no cells; 0.5 = <10 cells; 1 = 10-50 cells; 2 = 50-90 cells and 3 = >100 cells (and standard error, SE).

Table 2 Scores of the immunofluorescence analyses for the collagenase, inflammatory and bone formation markers evaluated. The scoring system adopted was the following: -, when less than 10% positivity was detected; +, for ≥10% positive cells; ++, for ≥25% positive cells and +++, for ≥50% positive cells.

Parameters	7 days	14 days	30 days
General tissue reaction			
Fibrosis	-	-	+
Fatty infiltrate	-	+	+
Hemorrhage	++	++	+
Necrosis	-	-	-
Degeneration	-	-	-
Foreign debris	-	-	-
Number of blood vessels (SE)	1.13 (1.55)	7.50 (3.42)	11 (11.38)
Specific tissue reaction (score 0-3 and SE)			
Polymorphonuclear leukocytes	0.38 (0.58)	0.25 (0.44)	0.25 (0.53)
Lympocytes	0.17 (0.38)	0.58 (0.65)	0.42 (0.58)
Eosinophils	0.04 (0.20)	-	-
Plasma cells	-	-	-
Macrophages	0.04 (0.20)	0.08 (0.28)	0.04 (0.20)
Multinucleated giant cells	-	-	-

Table 1

	7 days		14 days		30 days	
	Defect	*Membrane*	*Defect*	*Membrane*	*Defect*	*Membrane*
Collagenase activity						
MMP-1	-	-	+	++	++	+++
MMP-8	-	-	-	++	+	++
TIMP-1	-	-	+	+	++	+
Inflammation						
TNF-a	-	-	-	-	-	-
IL-1b	-	-	-	-	-	-
Bone formation						
Osteopontin	-	-	+	-	+	++
Osteocalcin	-	-	+	+	++	+
Bone sialoprotein	-	-	++	++	++	++
Mesenchymal cell marker						
Vimentin	-	-	+	-	-	+

Table 2
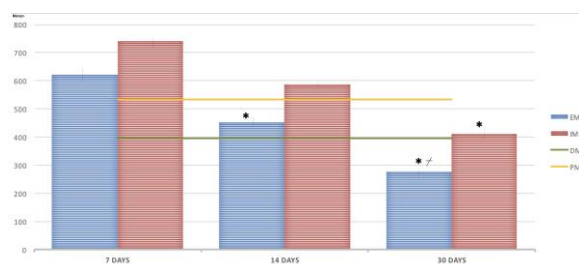
Figure 1
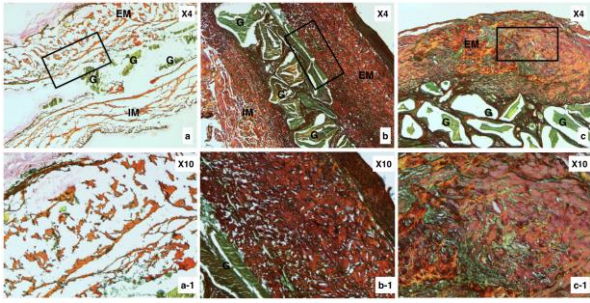
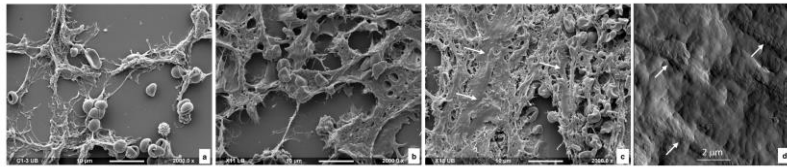**Figure 2**
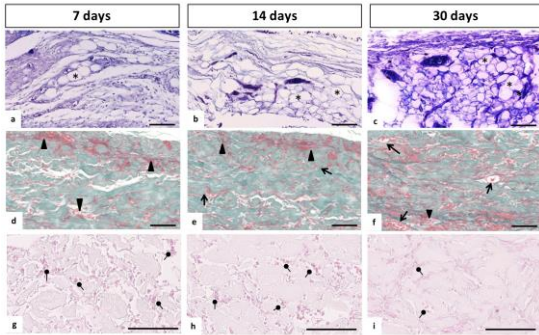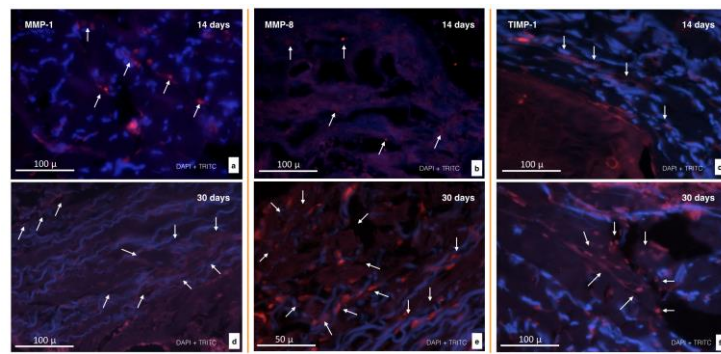

Figure 3

Figure 4
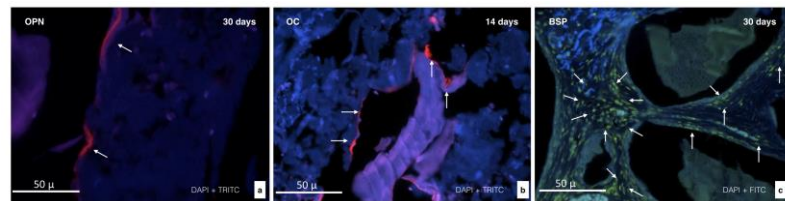

Figure 5

Figure 6

References

(1)   Melcher AH. On the repair potential of periodontal tissues. *J Periodontol* 1976; **47**: 256-260.

(2)   Calciolari E, Mardas N, Dereka X, Anagnostopoulos AK, Tsangaris GT, Donos N. Protein expression during early stages of bone regeneration under hydrophobic and hydrophilic titanium domes. A pilot study. *J Periodontal Res* 2017.

(3)   Mardas N, Chadha V, Donos N. Alveolar ridge preservation with guided bone regeneration and a synthetic bone substitute or a bovine-derived xenograft: a randomized, controlled clinical trial. *Clin Oral Implants Res* 2010; **21**: 688-698.

(4)   Retzepi M, Calciolari E, Wall I, Lewis MP, Donos N. The effect of experimental diabetes and glycaemic control on guided bone regeneration: histology and gene expression analyses. *Clin Oral Implants Res* 2017.

(5)   Al-Kattan R, Retzepi M, Calciolari E, Donos N. Microarray gene expression during early healing of GBR-treated calvarial critical size defects. *Clin Oral Implants Res* 2017; **28**: 1248-1257.

(6)   Retzepi M, Donos N. Guided Bone Regeneration: biological principle and therapeutic applications. *Clin Oral Implants Res* 2010; **21**: 567-576.

(7)   Donos N, Dereka X, Mardas N. Experimental models for guided bone regeneration in healthy and medically compromised conditions. *Periodontology 2000* 2015; **68**: 99-121.

(8)   Rakhmatia YD, Ayukawa Y, Furuhashi A, Koyano K. Current barrier membranes: titanium mesh and other membranes for guided bone regeneration in dental applications. *J Prosthodont Res* 2013; **57**: 3-14.

(9)   Shoulders MD, Raines RT. Collagen structure and stability. *Annu Rev Biochem* 2009; **78**: 929-958.

(10)   Bottino MC, Thomas V, Schmidt G, et al. Recent advances in the development of GTR/GBR membranes for periodontal regeneration--a materials perspective. *Dent Mater* 2012; **28**: 703-721.

(11)   Kim SH, Kim DY, Kim KH, Ku Y, Rhyu IC, Lee YM. The efficacy of a double-layer collagen membrane technique for overlaying block grafts in a rabbit calvarium model. *Clin Oral Implants Res* 2009; **20**: 1124-1132.

(12)   Kozlovsky A, Aboodi G, Moses O, et al. Bio-degradation of a resorbable collagen membrane (Bio-Gide) applied in a double-layer technique in rats. *Clin Oral Implants Res* 2009; **20**: 1116-1123.

(13)   Gielkens PF, Bos RR, Raghoebar GM, Stegenga B. Is there evidence that barrier membranes prevent bone resorption in autologous bone grafts during the healing period? A systematic review. *Int J Oral Maxillofac Implants* 2007; **22**: 390-398.

(14)   Hurzeler MB, Kohal RJ, Naghshbandi J, et al. Evaluation of a new bioresorbable barrier to facilitate guided bone regeneration around exposed implant threads. An experimental study in the monkey. *Int J Oral Maxillofac Surg* 1998; **27**: 315-320.

(15)   Kostopoulos L, Karring T. Augmentation of the rat mandible using guided tissue regeneration. *Clin Oral Implants Res* 1994; **5**: 75-82.

(16)   von Arx T, Broggini N, Jensen SS, Bornstein MM, Schenk RK, Buser D. Membrane durability and tissue response of different bioresorbable barrier membranes: a histologic study in the rabbit calvarium. *Int J Oral Maxillofac Implants* 2005; **20**: 843-853.

(17)   Zhao S, Pinholt EM, Madsen JE, Donath K. Histological evaluation of different biodegradable and non-biodegradable membranes implanted subcutaneously in rats. *J Craniomaxillofac Surg* 2000; **28**: 116-122.

(18)   Rothamel D, Schwarz F, Fienitz T, et al. Biocompatibility and biodegradation of a native porcine pericardium membrane: results of in vitro and in vivo examinations. *Int J Oral Maxillofac Implants* 2012; **27**: 146-154.

(19)   Schlegel AK, Mohler H, Busch F, Mehl A. Preclinical and clinical studies of a collagen membrane (Bio-Gide). *Biomaterials* 1997; **18**: 535-538.

(20)   Bozkurt A, Apel C, Sellhaus B, et al. Differences in degradation behavior of two non-cross-linked collagen barrier membranes: an in vitro and in vivo study. *Clin Oral Implants Res* 2014; **25**: 1403-1411.

(21)   Rothamel D, Schwarz F, Sager M, Herten M, Sculean A, Becker J. Biodegradation of differently cross-linked collagen membranes: an experimental study in the rat. *Clin Oral Implants Res* 2005; **16**: 369-378.

(22)   Moses O, Vitrial D, Aboodi G, et al. Biodegradation of three different collagen membranes in the rat calvarium: a comparative study. *J Periodontol* 2008; **79**: 905-911.

(23)   Calciolari E, Mardas N, Dereka X, Kostomitsopoulos N, Petrie A, Donos N. The effect of experimental osteoporosis on bone regeneration: Part 1, histology findings. *Clin Oral Implants Res* 2017; **28**: e101-e110.

(24)   Calciolari E, Mardas N, Dereka X, Anagnostopoulos AK, Tsangaris GT, Donos N. The effect of experimental osteoporosis on bone regeneration: part 2, proteomics results. *Clin Oral Implants Res* 2017; **28**: e135-e145.

(25)   Kilkenny C, Browne WJ, Cuthill IC, Emerson M, Altman DG. Improving Bioscience Research Reporting: The ARRIVE Guidelines for Reporting Animal Research. *PLoS Biol* 2010; **8**: e1000412.

(26)   Junqueira LC, Bignolas G, Brentani RR. Picrosirius staining plus polarization microscopy, a specific method for collagen detection in tissue sections. *Histochem J* 1979; **11**: 447-455.

(27)   Sulzbacher I, Birner P, Trieb K, Pichlbauer E, Lang S. The expression of bone morphogenetic proteins in osteosarcoma and its relevance as a prognostic parameter. *J Clin Pathol* 2002; **55**: 381-385.

(28)   Silva EC, Omonte SV, Martins AG, et al. Hyaluronic acid on collagen membranes: An experimental study in rats. *Arch Oral Biol* 2017; **73**: 214-222.

(29)   Schwarz F, Rothamel D, Herten M, Sager M, Becker J. Angiogenesis pattern of native and cross-linked collagen membranes: an immunohistochemical study in the rat. *Clin Oral Implants Res* 2006; **17**: 403-409.

(30)   Turri A, Elgali I, Vazirisani F, et al. Guided bone regeneration is promoted by the molecular events in the membrane compartment. *Biomaterials* 2016; **84**: 167-183.

(31)   Webster NL, Crowe SM. Matrix metalloproteinases, their production by monocytes and macrophages and their potential role in HIV-related diseases. *J Leukoc Biol* 2006; **80**: 1052-1066.

(32)   Bode W, Fernandez-Catalan C, Grams F, et al. Insights into MMP-TIMP interactions. *Ann N Y Acad Sci* 1999; **878**: 73-91.

(33)   Arumugam S, Jang YC, Chen-Jensen C, Gibran NS, Isik FF. Temporal activity of plasminogen activators and matrix metalloproteinases during cutaneous wound repair. *Surgery* 1999; **125**: 587-593.

(34) Bode W, Fernandez-Catalan C, Tschesche H, Grams F, Nagase H, Maskos K. Structural properties of matrix metalloproteinases. *Cell Mol Life Sci* 1999; **55**: 639-652.

(35) Kelley MJ, Rose AY, Song K, et al. Synergism of TNF and IL-1 in the induction of matrix metalloproteinase-3 in trabecular meshwork. *Invest Ophthalmol Vis Sci* 2007; **48**: 2634-2643.

(36) Philips N, Keller T, Gonzalez S. TGF beta-like regulation of matrix metalloproteinases by anti-transforming growth factor-beta, and anti-transforming growth factor-beta 1 antibodies in dermal fibroblasts: Implications for wound healing. *Wound Repair Regen* 2004; **12**: 53-59.

(37) Shi SR, Key ME, Kalra KL. Antigen retrieval in formalin-fixed, paraffin-embedded tissues: an enhancement method for immunohistochemical staining based on microwave oven heating of tissue sections. *The journal of histochemistry and cytochemistry : official journal of the Histochemistry Society* 1991; **39**: 741-748.

(38) Xie R, Chung JY, Ylaya K, et al. Factors influencing the degradation of archival formalin-fixed paraffin-embedded tissue sections. *The journal of histochemistry and cytochemistry : official journal of the Histochemistry Society* 2011; **59**: 356-365.

(39) Hatori K, Sasano Y, Takahashi I, Kamakura S, Kagayama M, Sasaki K. Osteoblasts and osteocytes express MMP2 and -8 and TIMP1, -2, and -3 along with extracellular matrix molecules during appositional bone formation. *Anat Rec A Discov Mol Cell Evol Biol* 2004; **277**: 262-271.

(40) Elgali I, Turri A, Xia W, et al. Guided bone regeneration using resorbable membrane and different bone substitutes: Early histological and molecular events. *Acta biomaterialia* 2016; **29**: 409-423.

(41) Hammerle CH, Jung RE, Yaman D, Lang NP. Ridge augmentation by applying bioresorbable membranes and deproteinized bovine bone mineral: a report of twelve consecutive cases. *Clin Oral Implants Res* 2008; **19**: 19-25.

(42) Zitzmann NU, Naef R, Scharer P. Resorbable versus nonresorbable membranes in combination with Bio-Oss for guided bone regeneration. *Int J Oral Maxillofac Implants* 1997; **12**: 844-852.

(43) Esposito M, Grusovin MG, Coulthard P, Worthington HV. The efficacy of various bone augmentation procedures for dental implants: a Cochrane systematic review of randomized controlled clinical trials. *Int J Oral Maxillofac Implants* 2006; **21**: 696-710.

(44) Felice P, Marchetti C, Piattelli A, et al. Vertical ridge augmentation of the atrophic posterior mandible with interpositional block grafts: bone from the iliac crest versus bovine anorganic bone. *European journal of oral implantology* 2008; **1**: 183-198.

(45) Donos N, Lang NP, Karoussis IK, Bosshardt D, Tonetti M, Kostopoulos L. Effect of GBR in combination with deproteinized bovine bone mineral and/or enamel matrix proteins on the healing of critical-size defects. *Clin Oral Implants Res* 2004; **15**: 101-111.

(46) Donos N, Bosshardt D, Lang N, et al. Bone formation by enamel matrix proteins and xenografts: an experimental study in the rat ramus. *Clin Oral Implants Res* 2005; **16**: 140-146.

(47) Becker W, Becker BE, Berg L, Prichard J, Caffesse R, Rosenberg E. New attachment after treatment with root isolation procedures: report for treated Class III and Class II furcations and vertical osseous defects. *Int J Periodontics Restorative Dent* 1988; **8**: 8-23.

(48)   Buser D, Dula K, Hess D, Hirt HP, Belser UC. Localized ridge augmentation with autografts and barrier membranes. *Periodontology 2000* 1999; **19**: 151-163.

(49)   Schenk RK, Buser D, Hardwick WR, Dahlin C. Healing pattern of bone regeneration in membrane-protected defects: a histologic study in the canine mandible. *Int J Oral Maxillofac Implants* 1994; **9**: 13-29.

(50)   Buser D, Chappuis V, Kuchler U, et al. Long-term stability of early implant placement with contour augmentation. *J Dent Res* 2013; **92**: 176S-182S.

(51)   Tal H, Kozlovsky A, Artzi Z, Nemcovsky CE, Moses O. Long-term bio-degradation of cross-linked and non-cross-linked collagen barriers in human guided bone regeneration. *Clin Oral Implants Res* 2008; **19**: 295-302.

(52)   Zohar R, Nemcovsky CE, Kebudi E, Artzi Z, Tal H, Moses O. Tetracycline impregnation delays collagen membrane degradation in vivo. *J Periodontol* 2004; **75**: 1096-1101.

(53)   Moses O, Nemcovsky CE, Tal H, Zohar R. Tetracycline modulates collagen membrane degradation in vitro. *J Periodontol* 2001; **72**: 1588-1593.

(54)   Moses O, Shemesh A, Aboodi G, Tal H, Weinreb M, Nemcovsky CE. Systemic tetracycline delays degradation of three different collagen membranes in rat calvaria. *Clin Oral Implants Res* 2009; **20**: 189-195.

(55)   Chu C, Deng J, Sun X, Qu Y, Man Y. Collagen Membrane and Immune Response in Guided Bone Regeneration: Recent Progress and Perspectives. *Tissue Eng Part B Rev* 2017.

(56)   Donos N, Mardas N, Chadha V. Clinical outcomes of implants following lateral bone augmentation: systematic assessment of available options (barrier membranes, bone grafts, split osteotomy). *J Clin Periodontol* 2008; **35**: 173-202.

(57)   Wang HL, Yuan K, Burgett F, Shyr Y, Syed S. Adherence of oral microorganisms to guided tissue membranes: an in vitro study. *J Periodontol* 1994; **65**: 211-218.

(58)   De Sanctis M, Zucchelli G, Clauser C. Bacterial colonization of bioabsorbable barrier material and periodontal regeneration. *J Periodontol* 1996; **67**: 1193-1200.

(59)   Tal H, Kozlovsky A, Artzi Z, Nemcovsky CE, Moses O. Cross-linked and non-cross-linked collagen barrier membranes disintegrate following surgical exposure to the oral environment: a histological study in the cat. *Clin Oral Implants Res* 2008; **19**: 760-766.

(60)   Donos N, Kostopoulos L, Karring T. Alveolar ridge augmentation by combining autogenous mandibular bone grafts and non-resorbable membranes. *Clin Oral Implants Res* 2002; **13**: 185-191.

(61)   Donos N, Kostopoulos L, Karring T. Alveolar ridge augmentation using a resorbable copolymer membrane and autogenous bone grafts. An experimental study in the rat. *Clin Oral Implants Res* 2002; **13**: 203-213.